Letter

Quantum jumps in driven-dissipative disordered many-body systems

Sparsh Gupta,[1,*] Hari Kumar Yadalam,[2,1,3,4,†] Manas Kulkarni,[1,‡] and Camille Aron[5,2,§]

[1]*International Centre for Theoretical Sciences, Tata Institute of Fundamental Research, 560089 Bangalore, India*

[2]*Laboratoire de Physique de l'École Normale Supérieure, ENS, Université PSL, CNRS, Sorbonne Université, Université Paris Cité, F-75005 Paris, France*

[3]*Department of Chemistry, University of California, Irvine, California 92614, USA*

[4]*Department of Physics and Astronomy, University of California, Irvine, California 92614, USA*

[5]*Institute of Physics, École Polytechnique Fédérale de Lausanne (EPFL), CH-1015 Lausanne, Switzerland*

(Received 2 January 2024; accepted 11 April 2024; published 6 May 2024)

We discuss how quantum jumps affect localized regimes in driven-dissipative disordered many-body systems featuring a localization transition. We introduce a deformation of the Lindblad master equation that interpolates between the standard Lindblad and the no-jump non-Hermitian dynamics of open quantum systems. As a platform, we use a disordered chain of hard-core bosons with nearest-neighbor interactions and subject to incoherent drive and dissipation at alternate sites. We probe both the statistics of complex eigenvalues of the deformed Liouvillian and dynamical observables of physical relevance. We show that reducing the number of quantum jumps, achievable through realistic postselection protocols, can promote the emergence of the localized phase. Our findings are based on exact diagonalization and time-dependent matrix-product state techniques.

DOI: 10.1103/PhysRevA.109.L050201

Introduction. Sufficiently strong disorder can markedly hinder the dynamics of many-body systems. Quantum many-body localized regimes [1–5], wherein transport is completely arrested, have attracted considerable attention because their inability to thermalize evades the foundations of statistical mechanics [6–10]. The delocalized and localized regimes, at respectively weak and strong disorder, are commonly probed by means of spectral [11,12] and dynamical properties [13,14]. The eigenvalue statistics are generically expected to transition from Hermitian random-matrix to one-dimensional Poisson statistics as the strength of the disorder increases. The transport and information-spreading properties at strong disorder are expected to display signs of nonergodicity, such as dependence on initial conditions or logarithmic growth of entanglement [15,16]. Various experiments demonstrating localization transitions have been successfully conducted across different quantum many-body platforms [17–24].

The inevitable presence of an environment is expected to destabilize localized regimes, confining their existence to intermediate timescales before complete thermalization with the environment [26–35]. However, it has recently been demonstrated that nonequilibrium environments could sustain localization [36–42], sparking renewed interest in many-body localization in driven-dissipative settings. These are often described by non-Hermitian Hamiltonians, where the non-Hermiticity mimics the hybridization with reservoirs and can be interpreted in terms of postselection protocols [36–43]. A natural approach that does not rely on postselection interpretation and which can systematically incorporate the effects of Markovian environments is the standard Lindblad quantum master equation approach [44–46]. In this approach, the environment contributes to two types of processes: the ones that can be absorbed in a non-Hermitian Hamiltonian description, and others that can be interpreted in terms of quantum jumps [45–51]. Recently, frameworks bridging these two approaches have been developed [52–54]. They rely on suitable deformations of the standard Lindblad equation and can be experimentally motivated [55–58].

In this Letter, we question the precise role of quantum jumps on the fate of localized regimes by working with a disordered one-dimensional many-body system coupled to a gain-loss environment. See the schematic in Fig. 1. To that end, we first introduce a specific deformation of the standard Lindblad master equation that involves a parameter $\zeta \in [0, 1]$ dialing the strength of quantum jump terms all the way from the non-Hermitian Hamiltonian to the standard Lindblad description. Our analysis of the influence of quantum jumps on the complex spectrum as well as on the dynamics of the ζ-deformed Liouvillian demonstrates that fewer quantum jumps can result in the emergence of localization at lower disorder strengths. To put it another way, postselection can promote localization. We emphasize that this is not only a formal construction but it can also find an experimental realization with realistic faulty detectors.

ζ-deformed theory. The Markovian evolution of open quantum systems is generically described by the Lindblad equation $\partial_t \rho(t) = \mathcal{L}\rho(t)$, with the Liouvillian $\mathcal{L}_\star := -\mathrm{i}[H, \star] + \sum_\alpha [O_\alpha \star O_\alpha^\dagger - \{O_\alpha^\dagger O_\alpha, \star\}/2]$, where H is the Hermitian Hamiltonian of the system and the O_α's, with $\alpha = 1, \ldots, M$, are the jump operators in the M dissipative

*sparsh.gupta@icts.res.in
†hyadalam@uci.edu
‡manas.kulkarni@icts.res.in
§aron@ens.fr

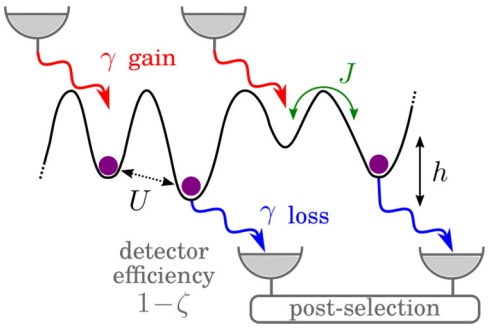

FIG. 1. Sketch of the disordered gain-loss model; see the Hamiltonian H in Eq. (3) and proposed protocol to implement the ζ-deformed Liouvillian $\mathcal{L}_\zeta$ in Eq. (2). Both gain and loss events are monitored by means of realistic detectors with efficiency $0 \leqslant 1-\zeta \leqslant 1$. Here, the postselection interpretation consists of selecting those monitored trajectories with no jump. See the Supplemental Material [25] for details and an alternative protocol.

channels. This Lindblad evolution can be unraveled into a quantum-jump trajectory ensemble as $\rho(t) = \sum_{n=0}^{\infty} \rho_n(t)$, where $\rho_n(t)$ is the conditional density matrix of the system subjected to precisely n quantum jumps until time t [45–51]. Let us introduce a weight $\zeta \in [0, 1]$ to each jump in a quantum trajectory. In analogy to the familiar terminology of the grand-canonical ensemble, we coin it the "quantum-jump fugacity." This defines a ζ-deformed ensemble where the density matrix $\rho_\zeta(t) = \sum_{n=0}^{\infty} \zeta^n \rho_n(t) / \sum_{n=0}^{\infty} \zeta^n \mathrm{Tr}[\rho_n(t)]$ evolves according to the following ζ-deformed Lindblad master equation,

$$\partial_t \rho_\zeta(t) = (\mathcal{L}_\zeta - \mathrm{Tr}[\mathcal{L}_\zeta \rho_\zeta(t)])\rho_\zeta(t), \tag{1}$$

where the ζ-deformed Liouvillian is given by

$$\mathcal{L}_\zeta \star := -\mathrm{i}[H, \star] + \sum_{\alpha=1}^{M} \left[\zeta O_\alpha \star O_\alpha^\dagger - \frac{1}{2}\{O_\alpha^\dagger O_\alpha, \star\} \right]. \tag{2}$$

The systematic and consistent construction of such a theory is detailed in the Supplemental Material [25]. The standard Lindblad equation is recovered in the limit $\zeta = 1$, whereas the limit $\zeta = 0$ corresponds to an evolution generated by the non-Hermitian Hamiltonian $\tilde{H} = H - \frac{\mathrm{i}}{2} \sum_{\alpha=1}^{M} O_\alpha^\dagger O_\alpha$. The subscript ζ in $\rho_\zeta(t)$ is to distinguish between the results of the deformed theory and those of the standard Lindblad evolution. The initial condition is given by $\rho_\zeta(0) = \rho(0)$ and the evolution in Eq. (1) is completely positive Hermiticity and trace preserving. The latter is ensured by the nonlinear trace term. The observables predicted from Eq. (1) can be experimentally measured by postselection protocols. In Fig. 1, we depict a possible protocol where both the quantum jumps due to gain and loss processes are monitored by means of detectors characterized by an efficiency $1-\zeta$; i.e., the error rate of returning a no-click result when a jump occurred is ζ. Here, the postselection protocol consists of discarding those trajectories where one or more jumps were monitored. Decreasing the efficiency of the detectors increases the average number of quantum jumps in the postselected dynamics. We discuss an alternative protocol in the Supplemental Material [25]. We note that generalized Lindblad equations of the type of Eq. (1) appear in the studies of full-counting statistics, where they are referred to as tilted or twisted master equations [59–61].

Disordered gain-loss model. To understand the role of quantum jumps on the localized-delocalized transition in non-Hermitian many-body systems, we consider a disordered gain-loss model defined by the following Hamiltonian (see Fig. 1),

$$H = \sum_{i=1}^{L} h_i n_i - J \sum_{i=1}^{L-1} (b_i^\dagger b_{i+1} + \mathrm{H.c.}) + U \sum_{i=1}^{L-1} n_i n_{i+1}, \tag{3}$$

with $n_i = b_i^\dagger b_i$, and by the on-site jump operators

$$O_i = \begin{cases} \sqrt{2\gamma}\, b_i^\dagger & \text{if } i \text{ is odd,} \\ \sqrt{2\gamma}\, b_i & \text{if } i \text{ is even.} \end{cases} \tag{4}$$

The $b_i^\dagger$'s and b_i's, $i = 1, \ldots, L$, are on-site creation and annihilation operators of hard-core bosons living on a one-dimensional lattice with L sites and open boundary conditions. The Hamiltonian in Eq. (3) is U(1) symmetric; i.e., it conserves the total number of particles $N = \sum_{i=1}^{L} n_i$. h_i are independent random energy levels uniformly distributed in the interval $[-h, h]$. J is the intersite hopping amplitude. U is the intersite interaction which we set to $U = 2J$ for the Hamiltonian to be equivalent to the disordered Heisenberg spin chain which has been extensively studied in the context of Hermitian many-body localization [11–14]. Its transition was found around $h^\star \approx 7J$ in our conventions. γ sets the rates of both the incoherent gain and loss occurring at alternating sites, which we set as $\gamma = 0.1J$ throughout this work. We choose J as the unit of energy and, therefore, we set $J = 1$. The corresponding ζ-deformed Liouvillian $\mathcal{L}_\zeta$ in Eq. (2) has a weak U(1) symmetry that corresponds to the conservation of the particle number difference between the bra and ket sides of the states upon acting with $\mathcal{L}_\zeta$; see details in the Supplemental Material [25].

In the limit of $\zeta = 0$, there is an additional weak U(1) symmetry of $\mathcal{L}_0$ that corresponds to conserving the particle number associated with the bra and ket independently. Moreover, the $\zeta = 0$ dynamics boils down to that of the non-Hermitian gain-loss Hamiltonian

$$\tilde{H} = H - \mathrm{i}\gamma \sum_{i=1}^{L} (-1)^i b_i^\dagger b_i, \quad \zeta = 0, \tag{5}$$

recently studied in Refs. [36,42,62]. $\tilde{H}$ also conserves the total number of particles. It displays a non-Hermitian many-body localization transition at $h^\star \approx 4.2$, manifesting itself as a crossover between $\mathrm{AI}^\dagger$ non-Hermitian random-matrix (weak disorder) and two-dimensional Poisson ensembles (strong disorder). Here, we explore this physics both from spectral and dynamical points of view in the general ζ-deformed Lindbladian framework that captures the effect of quantum jumps in a controllable fashion.

Spectral signatures. The Liouvillian $\mathcal{L}_\zeta$ in Eq. (2) is a non-Hermitian operator and we analyze its complex spectrum by means of exact diagonalization. We specifically compute the statistics of the complex spacing ratio [62] defined for each

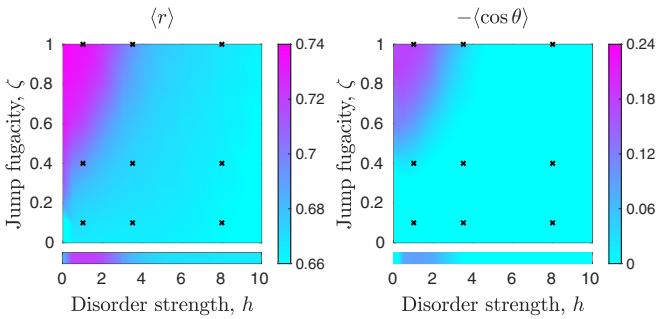

FIG. 2. Complex spacing ratios of the spectrum of $\mathcal{L}_\zeta$ in Eq. (2): (left) $\langle r\rangle$ and (right) $-\langle\cos\theta\rangle$ computed by exact diagonalization of a system of $L = 8$ sites, in the zero charge sector of the weak U(1) symmetry, and averaged over 160 disorder samples. The bottom strips are obtained using the non-Hermitian Hamiltonian $\tilde{H}$ (half-filling sector) in Eq. (5) for system size $L = 16$ averaged over 160 disorder samples. The nine black crosses in each panel correspond to the parameters at which the densities of complex spacing ratios are presented in Fig. 3.

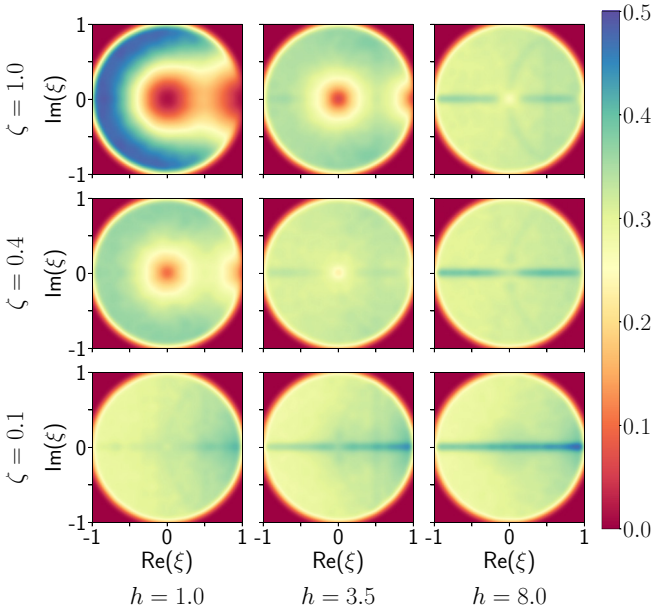

FIG. 3. Density of complex spacing ratio defined in Eq. (6) for representative values of disorder strength h and quantum-jump fugacity ζ for a system of $L = 8$ sites in the zero charge sector of the weak U(1) symmetry, and averaged over 160 disorder samples. The isotropy associated with the localized phase increases with decreasing ζ or increasing h.

eigenvalue z as

$$\xi = \frac{z^{\mathrm{NN}} - z}{z^{\mathrm{NNN}} - z} = re^{\mathrm{i}\theta}, \tag{6}$$

where z^{NN} and z^{NNN} are the nearest- and the next-nearest-neighbor eigenvalues to z (in euclidean distance), respectively. r and θ are respectively the norm and the argument of ξ. Note that the nonlinear trace term in $\mathcal{L}_\zeta$ simply adds a constant shift to the spectrum and is therefore inconsequential to level-spacing statistics. The statistics of ξ are indicative of the chaotic or regular nature of complex-valued spectra and have been studied in the context of non-Hermitian interacting disordered Hamiltonians [41,62,63] and open quantum systems described by standard Lindblad evolutions [62,64–69]. For chaotic systems, the eigenvalues experience level repulsion resulting in a vanishing complex spacing ratio distribution at small r and an anisotropic angular pattern. The distributions of r and θ are generically dictated by Ginibre random matrix ensembles, and their averages take the value $\langle r\rangle \approx 0.738$ and $-\langle\cos\theta\rangle \approx 0.244$. On the other hand, for uncorrelated energy levels, the complex spacing ratio is uniformly distributed inside a unit circle [62] with $\langle r\rangle = 2/3$ and $-\langle\cos\theta\rangle = 0$.

In Fig. 2, we present $\langle r\rangle$ and $-\langle\cos\theta\rangle$ as a function of both the disorder strength h and the quantum-jump fugacity ζ. The results are obtained from the zero-charge sector of the weak U(1) symmetry for a system of $L = 8$ sites and after averaging over 160 disorder samples. For the standard Lindblad evolution at $\zeta = 1$, we find a clear transition between random matrix predictions at weak disorder and two-dimensional Poisson predictions at strong disorder. When ζ is reduced, the location of this transition is shifted to lower disorder strengths: reducing the number of quantum jumps facilitates the emergence of localization. In the $\zeta = 0$ case, the additional weak U(1) symmetry is responsible for spurious statistics which are known to produce deceitful level attraction between eigenvalues of different symmetry sectors. We attribute the apparent loss of a delocalized phase in the vicinity of $\zeta = 0$ to a remnant of this extra symmetry. To circumvent this situation at $\zeta = 0$, one should resort to analyzing the spectrum of the non-Hermitian Hamiltonian [36,42,62] in Eq. (5). The corresponding results are presented in the strips of Fig. 2. In Fig. 3, we illustrate further these effects of disorder and quantum-jump fugacity by presenting representative plots of the density of complex spacing ratios ξ in Eq. (6) for different values of h and ζ. At strong disorder and weak fugacity, we find that this distribution is isotropic and homogeneous within the unit circle, which is a hallmark of integrable systems. On the other hand, for weak disorder and large fugacity, the distribution is found to be anisotropic and inhomogeneous, which is expected for chaotic systems.

Dynamical signatures. Strong disorder slows down the dynamics by raising the energetic barriers that suppress the intersite hopping. A hallmark of localized dynamics is the ever-lasting memory of their initial conditions. We choose to work with the charge density wave initial state $\rho(0) = |1, 0, \ldots, 1, 0\rangle\langle 1, 0, \ldots, 1, 0|$, which is a product state and a steady-state of the ζ-deformed gain-loss dynamics in the absence of particle hopping, $J = 0$. We numerically integrate the subsequent dynamics generated by Eq. (1) by employing a standard fourth-order Runge-Kutta algorithm (RK45). We quantify the fate of the staggered order present in the initial state $\rho(0)$ by computing the dynamics of the so-called imbalance [17,70]

$$\mathcal{I}(t) = \frac{\sum_{i=1}^{L}(-1)^{i+1}\mathrm{Tr}[b_i^\dagger b_i \rho_\zeta(t)]}{\sum_{i=1}^{L}\mathrm{Tr}[b_i^\dagger b_i \rho_\zeta(t)]}. \tag{7}$$

This is a directly observable quantity, $-1 \leqslant \mathcal{I}(t) \leqslant 1$, with $\mathcal{I}(t = 0) = 1$. Additionally, exploiting the formal analogy between full-counting statistics (FCS) in grand-canonical

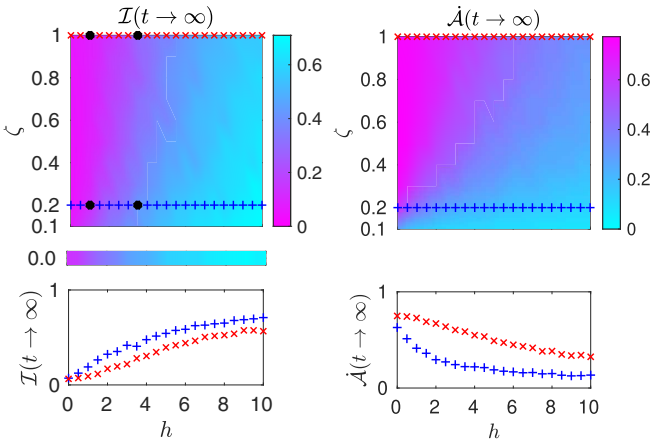

FIG. 4. (Left panel) Steady-state imbalance, $\mathcal{I}(t\to\infty)$ defined in Eq. (7), as a function of disorder strength h and quantum-jump-fugacity ζ. The lower strip corresponds to $\zeta = 0$. (Right panel) Steady-state rate of dynamical activity, $\dot{\mathcal{A}}(t\to\infty)$ defined in Eq. (8). The lower panels correspond to the cuts at $\zeta = 0.2$ and $\zeta = 1$ indicated in the upper panels. The dynamics are generated by Eq. (1). For imbalance (respectively, dynamical activity), we consider a system of $L = 10$ (respectively, $L = 8$) sites averaged over 100 (resppectively, 160) disorder samples. The four black dots in the upper left panel correspond to the parameters at which the transient time-dynamics are produced in Fig. 5.

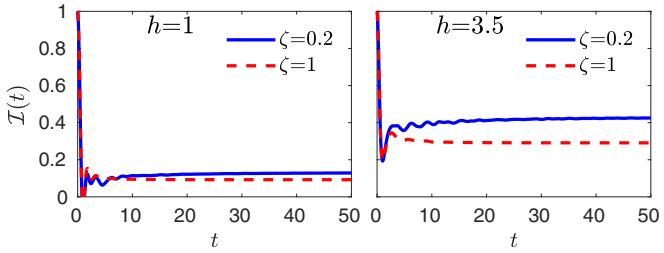

FIG. 5. Time dynamics of the imbalance $\mathcal{I}(t)$ defined in Eq. (7) for representative values of the quantum-jump fugacity ζ and the disorder strength h given in the legend. The data are produced by numerically exact integration of Eq. (1) for a system of $L = 10$ sites and averaged over 100 disorder samples.

ensembles [60] and the quantum trajectories ensemble interpretation of Lindblad dynamics [71,72], we monitor the rate of dynamical activity [72,73]

$$\dot{\mathcal{A}}(t) = \frac{1}{\zeta}\partial_t \langle n(t)\rangle_\zeta, \tag{8}$$

where $\langle n(t)\rangle_\zeta$ is the number of quantum jumps occurring between time $t = 0$ to t averaged over the quantum trajectories generated by $\mathcal{L}_\zeta$. For the standard Lindblad evolution $\zeta = 1$, the steady-state rate of dynamical activity is directly related to the imbalance as $\dot{\mathcal{A}}(t\to\infty) = \gamma L[1 - \mathcal{I}(t\to\infty)]$. For $\zeta < 1$, $\dot{\mathcal{A}}(t\to\infty)$ involves additional contributions from two-time jump correlations. Details of this connection to FCS are provided in the Supplemental Material [25].

In Fig. 4, we present both the steady-state imbalance $\mathcal{I}(t\to\infty)$ and the rate of dynamical activity $\dot{\mathcal{A}}(t\to\infty)$ as a function of the disorder strength h and the quantum-jump fugacity ζ. The results are consistent with those obtained from spectral statistics. For the standard Lindblad evolution $\zeta = 1$, we find a clear transition from a steady state with vanishing imbalance and a finite rate of dynamical activity at weak disorder to a steady state with imbalance close to unity and a vanishing rate of activity. When ζ is reduced, the location of this transition is shifted to lower disorder strengths, confirming once again that quantum jumps tend to destabilize the localized regime. Contrary to the results of the spectral statistics above, these dynamical indicators are not prone to subtleties involving symmetry sectors. At finite but very small ζ, the time it takes to reach the steady state diverges since the typical timescale between two jumps can be roughly estimated to be $\tau \sim 1/\gamma\zeta$. Indeed, the limits $t\to\infty$ and $\zeta\to 0$ are generically not expected to commute. This results in significant numerical challenges in capturing the steady state and we do not provide data in the regime $\zeta \ll 1$. To better illustrate the influence of the disorder strength h and the quantum-jump fugacity ζ, the lower panels of Fig. 4 show the steady-state imbalance and rate of dynamical activity as a function of h for two representative values of ζ.

In Fig. 5, we show the transient dynamics of imbalance from the initial state till the steady state for representative values of the disorder strength h and the quantum-jump fugacity ζ. The steady-state values increase with h and decrease with ζ. The timescale of the approach to the steady state is dictated by the inverse of the minimum Liouvillian gap [74]. We have used this spectral information to ensure the convergence of all steady-state results presented in this Letter. While the system sizes presented so far, up to $L = 10$, are state-of-the-art when it comes to exactly computing the dynamics of open quantum systems, they are still relatively small owing to the challenges posed by numerical time integration. To firmly assert the influence of quantum jumps on the localized regime, we resort to a time-dependent matrix product state (MPS) technique that allows us to reach much larger system sizes, up to $L = 32$. In practice, we implemented a time-evolving block decimation of a matrix product density operator representation of the ζ-deformed Lindblad evolution in Eq. (1). See the Supplementaal Material [25] for details. The results are averaged over 100 disorder samples. This technique produces reliable results deep in the localized regime and we work at $h = 20$ where convergence is achieved with a maximal bond dimension of $\chi = 2^7$. In Fig. 6, we show the transient dynamics of the imbalance from the initial state till the steady state for representative values of the quantum-jump fugacity ζ. The MPS results entirely validate the previous results obtained by numerically exact integration of systems of smaller sizes.

Conclusion and discussion. We started from a disordered many-body system that already exhibited a localized regime and found that postselection protocols can facilitate localization at lower disorder strengths. This is different from the measurement-induced phase transitions [75–77] where repeated measurements can localize featureless systems, such as random unitary circuits [78] or free fermions [79], but are facing a major experimental challenge as they rely on generating and recording a large number of measurement trajectories. In our case, the ζ-deformed Lindblad offers both a spectral and a dynamical window into the localized phase. This approach

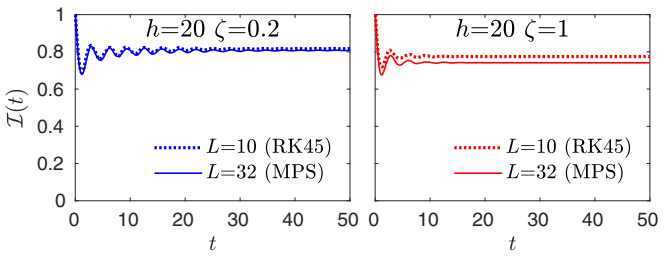

FIG. 6. Time dynamics of the imbalance $\mathcal{I}(t)$ for a very large system, $L = 32$, deep in the localized regime, $h = 20$, and for representative values of the quantum-jump fugacity ζ given in the legend. The data are produced by means of the time-dependent matrix product state (MPS) technique and averaged over 100 disorder samples. The dashed lines correspond to the results obtained by numerically exact integration of Eq. (1) for a system of $L = 10$ sites.

not only harnesses standard methods of full counting statistics to the study of Lindblad dynamics but it is also physically realizable by means of realistic postselection protocols in quantum optical setups. It can easily be adapted to other systems of interest in condensed matter and quantum optics, such as open quantum spin chains and driven-dissipative Jaynes-Cummings Hubbard systems, to name a few.

Acknowledgments. We thank F. Minganti and F. Ferrari for useful discussions. H.K.Y., C.A., and M.K. are grateful for the support from Project No. 6004-1 of the Indo-French Centre for the Promotion of Advanced Research (IFCPAR). M.K. acknowledges supportfrom a SERB Matrics Grant (Grant No. MTR/2019/001101) and the SERB VAJRA faculty scheme (Grant No. VJR/2019/000079). M.K. acknowledges support from the Department of Atomic Energy, Government of India, under Project No. RTI4001. C.A. acknowledges support from the French ANR, "MoMA" Project No. ANR-19-CE30-0020. M.K. is grateful for the hospitality of the École Normale Supérieure (Paris) and the École Polytechnique Fédérale de Lausanne. S.G. and H.K.Y. have equally contributed to producing the numerical data presented in this work.

[1] L. Fleishman and P. W. Anderson, Interactions and the Anderson transition, Phys. Rev. B **21**, 2366 (1980).
[2] B. L. Altshuler, Y. Gefen, A. Kamenev, and L. S. Levitov, Quasiparticle lifetime in a finite system: A nonperturbative approach, Phys. Rev. Lett. **78**, 2803 (1997).
[3] D. Basko, I. Aleiner, and B. Altshuler, Metal-insulator transition in a weakly interacting many-electron system with localized single-particle states, Ann. Phys. **321**, 1126 (2006).
[4] R. Nandkishore and D. A. Huse, Many-body localization and thermalization in quantum statistical mechanics, Annu. Rev. Condens. Matter Phys. **6**, 15 (2015).
[5] F. Alet and N. Laflorencie, Many-body localization: An introduction and selected topics, C. R. Phys. **19**, 498 (2018).
[6] J. M. Deutsch, Quantum statistical mechanics in a closed system, Phys. Rev. A **43**, 2046 (1991).
[7] M. Srednicki, Chaos and quantum thermalization, Phys. Rev. E **50**, 888 (1994).
[8] M. Rigol, V. Dunjko, and M. Olshanii, Thermalization and its mechanism for generic isolated quantum systems, Nature (London) **452**, 854 (2008).
[9] L. D'Alessio, Y. Kafri, A. Polkovnikov, and M. Rigol, From quantum chaos and eigenstate thermalization to statistical mechanics and thermodynamics, Adv. Phys. **65**, 239 (2016).
[10] J. M. Deutsch, Eigenstate thermalization hypothesis, Rep. Prog. Phys. **81**, 082001 (2018).
[11] V. Oganesyan and D. A. Huse, Localization of interacting fermions at high temperature, Phys. Rev. B **75**, 155111 (2007).
[12] A. Pal and D. A. Huse, Many-body localization phase transition, Phys. Rev. B **82**, 174411 (2010).
[13] D. A. Abanin and Z. Papić, Recent progress in many-body localization, Ann. Phys. **529**, 1700169 (2017).
[14] D. A. Abanin, E. Altman, I. Bloch, and M. Serbyn, Colloquium: Many-body localization, thermalization, and entanglement, Rev. Mod. Phys. **91**, 021001 (2019).
[15] J. H. Bardarson, F. Pollmann, and J. E. Moore, Unbounded growth of entanglement in models of many-body localization, Phys. Rev. Lett. **109**, 017202 (2012).
[16] M. Serbyn, Z. Papić, and D. A. Abanin, Universal slow growth of entanglement in interacting strongly disordered systems, Phys. Rev. Lett. **110**, 260601 (2013).
[17] M. Schreiber, S. S. Hodgman, P. Bordia, H. P. Lüschen, M. H. Fischer, R. Vosk, E. Altman, U. Schneider, and I. Bloch, Observation of many-body localization of interacting fermions in a quasirandom optical lattice, Science **349**, 842 (2015).
[18] J. Smith, A. Lee, P. Richerme, B. Neyenhuis, P. W. Hess, P. Hauke, M. Heyl, D. A. Huse, and C. Monroe, Many-body localization in a quantum simulator with programmable random disorder, Nat. Phys. **12**, 907 (2016).
[19] J.-y. Choi, S. Hild, J. Zeiher, P. Schauß, A. Rubio-Abadal, T. Yefsah, V. Khemani, D. A. Huse, I. Bloch, and C. Gross, Exploring the many-body localization transition in two dimensions, Science **352**, 1547 (2016).
[20] P. Roushan, C. Neill, J. Tangpanitanon, V. M. Bastidas, A. Megrant, R. Barends, Y. Chen, Z. Chen, B. Chiaro, A. Dunsworth *et al.*, Spectroscopic signatures of localization with interacting photons in superconducting qubits, Science **358**, 1175 (2017).
[21] K. Xu, J.-J. Chen, Y. Zeng, Y.-R. Zhang, C. Song, W. Liu, Q. Guo, P. Zhang, D. Xu, H. Deng, K. Huang, H. Wang, X. Zhu, D. Zheng, and H. Fan, Emulating many-body localization with a superconducting quantum processor, Phys. Rev. Lett. **120**, 050507 (2018).
[22] K. X. Wei, C. Ramanathan, and P. Cappellaro, Exploring localization in nuclear spin chains, Phys. Rev. Lett. **120**, 070501 (2018).
[23] A. Lukin, M. Rispoli, R. Schittko, M. E. Tai, A. M. Kaufman, S. Choi, V. Khemani, J. Léonard, and M. Greiner, Probing entanglement in a many-body–localized system, Science **364**, 256 (2019).
[24] M. Gong, G. D. de Moraes Neto, C. Zha, Y. Wu, H. Rong, Y. Ye, S. Li, Q. Zhu, S. Wang, Y. Zhao, F. Liang, J. Lin, Y. Xu, C.-Z. Peng, H. Deng, A. Bayat, X. Zhu, and J.-W. Pan, Experimental characterization of the quantum many-body localization transition, Phys. Rev. Res. **3**, 033043 (2021).

[25] See Supplemental Material at http://link.aps.org/supplemental/10.1103/PhysRevA.109.L050201 for details on the ζ-deformed theory, the connection to FCS, the symmetries of $\mathcal{L}_\zeta$, the equations of motion for population and imbalance, and the TEBD-MPDO solver, which includes Refs. [36,39,44–52,54,80–94].

[26] M. H. Fischer, M. Maksymenko, and E. Altman, dynamics of a many-body-localized system coupled to a bath, Phys. Rev. Lett. **116**, 160401 (2016).

[27] M. V. Medvedyeva, T. Prosen, and M. Žnidarič, Influence of dephasing on many-body localization, Phys. Rev. B **93**, 094205 (2016).

[28] B. Everest, I. Lesanovsky, J. P. Garrahan, and E. Levi, Role of interactions in a dissipative many-body localized system, Phys. Rev. B **95**, 024310 (2017).

[29] I. Vakulchyk, I. Yusipov, M. Ivanchenko, S. Flach, and S. Denisov, Signatures of many-body localization in steady states of open quantum systems, Phys. Rev. B **98**, 020202(R) (2018).

[30] E. van Nieuwenburg, J. Y. Malo, A. Daley, and M. Fischer, Dynamics of many-body localization in the presence of particle loss, Quantum Sci. Technol. **3**, 01LT02 (2018).

[31] Z. Lenarčič, O. Alberton, A. Rosch, and E. Altman, Critical behavior near the many-body localization transition in driven open systems, Phys. Rev. Lett. **125**, 116601 (2020).

[32] P. Kos, T. Prosen, and B. Bertini, Thermalization dynamics and spectral statistics of extended systems with thermalizing boundaries, Phys. Rev. B **104**, 214303 (2021).

[33] J. Mák, M. J. Bhaseen, and A. Pal, Statics and dynamics of non-Hermitian many-body localization, Commun. Phys. **7**, 92 (2024).

[34] H. P. Lüschen, P. Bordia, S. S. Hodgman, M. Schreiber, S. Sarkar, A. J. Daley, M. H. Fischer, E. Altman, I. Bloch, and U. Schneider, Signatures of many-body localization in a controlled open quantum system, Phys. Rev. X **7**, 011034 (2017).

[35] A. Rubio-Abadal, J.-y. Choi, J. Zeiher, S. Hollerith, J. Rui, I. Bloch, and C. Gross, Many-body delocalization in the presence of a quantum bath, Phys. Rev. X **9**, 041014 (2019).

[36] R. Hamazaki, K. Kawabata, and M. Ueda, Non-Hermitian many-body localization, Phys. Rev. Lett. **123**, 090603 (2019).

[37] A. Panda and S. Banerjee, Entanglement in nonequilibrium steady states and many-body localization breakdown in a current-driven system, Phys. Rev. B **101**, 184201 (2020).

[38] L.-J. Zhai, S. Yin, and G.-Y. Huang, Many-body localization in a non-Hermitian quasiperiodic system, Phys. Rev. B **102**, 064206 (2020).

[39] K. Yamamoto, M. Nakagawa, M. Tezuka, M. Ueda, and N. Kawakami, Universal properties of dissipative Tomonaga-Luttinger liquids: Case study of a non-Hermitian XXZ spin chain, Phys. Rev. B **105**, 205125 (2022).

[40] C. M. Dai, Y. Zhang, and X. X. Yi, Dynamical localization in non-Hermitian quasicrystals, Phys. Rev. A **105**, 022215 (2022).

[41] K. Suthar, Y.-C. Wang, Y.-P. Huang, H. H. Jen, and J.-S. You, Non-Hermitian many-body localization with open boundaries, Phys. Rev. B **106**, 064208 (2022).

[42] S. Ghosh, S. Gupta, and M. Kulkarni, Spectral properties of disordered interacting non-Hermitian systems, Phys. Rev. B **106**, 134202 (2022).

[43] Y. Ashida, Z. Gong, and M. Ueda, Non-Hermitian physics, Adv. Phys. **69**, 249 (2020).

[44] H.-P. Breuer and F. Petruccione, *The Theory of Open Quantum Systems* (Oxford University Press, Oxford, 2002).

[45] H. J. Carmichael, *An Open Systems Approach to Quantum Optics* (Springer-Verlag, Berlin, 1993).

[46] A. J. Daley, Quantum trajectories and open many-body quantum systems, Adv. Phys. **63**, 77 (2014).

[47] J. Dalibard, Y. Castin, and K. Mølmer, Wave-function approach to dissipative processes in quantum optics, Phys. Rev. Lett. **68**, 580 (1992).

[48] K. Mølmer, Y. Castin, and J. Dalibard, Monte Carlo wave-function method in quantum optics, J. Opt. Soc. Am. B **10**, 524 (1993).

[49] R. Dum, P. Zoller, and H. Ritsch, Monte Carlo simulation of the atomic master equation for spontaneous emission, Phys. Rev. A **45**, 4879 (1992).

[50] K. Mølmer and Y. Castin, Monte Carlo wave functions in quantum optics, Quantum Semiclass. Opt. **8**, 49 (1996).

[51] M. B. Plenio and P. L. Knight, The quantum-jump approach to dissipative dynamics in quantum optics, Rev. Mod. Phys. **70**, 101 (1998).

[52] K. G. Zloshchastiev and A. Sergi, Comparison and unification of non-Hermitian and Lindblad approaches with applications to open quantum optical systems, J. Mod. Opt. **61**, 1298 (2014).

[53] F. Minganti, A. Miranowicz, R. W. Chhajlany, and F. Nori, Quantum exceptional points of non-Hermitian Hamiltonians and Liouvillians: The effects of quantum jumps, Phys. Rev. A **100**, 062131 (2019).

[54] F. Minganti, A. Miranowicz, R. W. Chhajlany, I. I. Arkhipov, and F. Nori, Hybrid-Liouvillian formalism connecting exceptional points of non-Hermitian Hamiltonians and Liouvillians via postselection of quantum trajectories, Phys. Rev. A **101**, 062112 (2020).

[55] J. C. Bergquist, R. G. Hulet, W. M. Itano, and D. J. Wineland, Observation of quantum jumps in a single atom, Phys. Rev. Lett. **57**, 1699 (1986).

[56] T. Sauter, W. Neuhauser, R. Blatt, and P. E. Toschek, Observation of quantum jumps, Phys. Rev. Lett. **57**, 1696 (1986).

[57] Z. K. Minev, S. O. Mundhada, S. Shankar, P. Reinhold, R. Gutiérrez-Jáuregui, R. J. Schoelkopf, M. Mirrahimi, H. J. Carmichael, and M. H. Devoret, To catch and reverse a quantum jump mid-flight, Nature (London) **570**, 200 (2019).

[58] W. Chen, M. Abbasi, Y. N. Joglekar, and K. W. Murch, Quantum jumps in the non-Hermitian dynamics of a superconducting qubit, Phys. Rev. Lett. **127**, 140504 (2021).

[59] M. Esposito, U. Harbola, and S. Mukamel, Nonequilibrium fluctuations, fluctuation theorems, and counting statistics in quantum systems, Rev. Mod. Phys. **81**, 1665 (2009).

[60] J. P. Garrahan and I. Lesanovsky, Thermodynamics of quantum jump trajectories, Phys. Rev. Lett. **104**, 160601 (2010).

[61] H. K. Yadalam, B. K. Agarwalla, and U. Harbola, Counting statistics of energy transport across squeezed thermal reservoirs, Phys. Rev. A **105**, 062219 (2022).

[62] L. Sá, P. Ribeiro, and T. Prosen, Complex spacing ratios: A signature of dissipative quantum chaos, Phys. Rev. X **10**, 021019 (2020).

[63] A. M. García-García, L. Sá, and J. J. M. Verbaarschot, Symmetry classification and universality in non-Hermitian many-body quantum chaos by the Sachdev-Ye-Kitaev model, Phys. Rev. X **12**, 021040 (2022).

[64] K. Wang, F. Piazza, and D. J. Luitz, Hierarchy of relaxation timescales in local random Liouvillians, Phys. Rev. Lett. **124**, 100604 (2020).

[65] A. Rubio-García, R. A. Molina, and J. Dukelsky, From integrability to chaos in quantum Liouvillians, SciPost Phys. Core **5**, 026 (2022).
[66] R. Hamazaki, M. Nakagawa, T. Haga, and M. Ueda, Lindbladian many-body localization, arXiv:2206.02984.
[67] I. Yusipov and M. Ivanchenko, Quantum Lyapunov exponents and complex spacing ratios: Two measures of dissipative quantum chaos, Chaos **32**, 043106 (2022).
[68] M. Prasad, H. K. Yadalam, C. Aron, and M. Kulkarni, Dissipative quantum dynamics, phase transitions, and non-Hermitian random matrices, Phys. Rev. A **105**, L050201 (2022).
[69] F. Ferrari, L. Gravina, D. Eeltink, P. Scarlino, V. Savona, and F. Minganti, Steady-state quantum chaos in open quantum systems, arXiv:2305.15479.
[70] P. Sierant and J. Zakrzewski, Challenges to observation of many-body localization, Phys. Rev. B **105**, 224203 (2022).
[71] G. Manzano and R. Zambrini, Quantum thermodynamics under continuous monitoring: A general framework, AVS Quantum Sci. **4**, 025302 (2022).
[72] G. T. Landi, M. J. Kewming, M. T. Mitchison, and P. P. Potts, Current fluctuations in open quantum systems: Bridging the gap between quantum continuous measurements and full counting statistics, PRX Quantum **5**, 020201 (2024).
[73] J. P. Garrahan, A. D. Armour, and I. Lesanovsky, Quantum trajectory phase transitions in the micromaser, Phys. Rev. E **84**, 021115 (2011).
[74] The Liouvillian gap is defined as minus the real part of the difference of eigenvalues with largest and next largest real parts.
[75] Y. Li, X. Chen, and M. P. A. Fisher, Measurement-driven entanglement transition in hybrid quantum circuits, Phys. Rev. B **100**, 134306 (2019).
[76] M. J. Gullans and D. A. Huse, Dynamical purification phase transition induced by quantum measurements, Phys. Rev. X **10**, 041020 (2020).
[77] A. Zabalo, M. J. Gullans, J. H. Wilson, S. Gopalakrishnan, D. A. Huse, and J. H. Pixley, Critical properties of the measurement-induced transition in random quantum circuits, Phys. Rev. B **101**, 060301(R) (2020).
[78] B. Skinner, J. Ruhman, and A. Nahum, Measurement-induced phase transitions in the dynamics of entanglement, Phys. Rev. X **9**, 031009 (2019).
[79] M. Buchhold, Y. Minoguchi, A. Altland, and S. Diehl, Effective theory for the measurement-induced phase transition of Dirac fermions, Phys. Rev. X **11**, 041004 (2021).
[80] M. Ferri-Cortés, J. A. Almanza-Marrero, R. López, R. Zambrini, and G. Manzano, Entropy production and fluctuation theorems for monitored quantum systems under imperfect detection, arXiv:2308.08491.
[81] U. Schollwöck, The density-matrix renormalization group in the age of matrix product states, Ann. Phys. **326**, 96 (2011).
[82] A. McDonald, R. Hanai, and A. A. Clerk, Nonequilibrium stationary states of quantum non-Hermitian lattice models, Phys. Rev. B **105**, 064302 (2022).
[83] D. Jaschke, S. Montangero, and L. D. Carr, One-dimensional many-body entangled open quantum systems with tensor network methods, Quantum Sci. Technol. **4**, 013001 (2018).
[84] H. Weimer, A. Kshetrimayum, and R. Orús, Simulation methods for open quantum many-body systems, Rev. Mod. Phys. **93**, 015008 (2021).
[85] T. Prosen and I. Pižorn, Operator space entanglement entropy in a transverse Ising chain, Phys. Rev. A **76**, 032316 (2007).
[86] G. Vidal, Efficient classical simulation of slightly entangled quantum computations, Phys. Rev. Lett. **91**, 147902 (2003).
[87] G. Vidal, Efficient simulation of one-dimensional quantum many-body systems, Phys. Rev. Lett. **93**, 040502 (2004).
[88] S. Paeckel, T. Köhler, A. Swoboda, S. R. Manmana, U. Schollwöck, and C. Hubig, Time-evolution methods for matrix-product states, Ann. Phys. **411**, 167998 (2019).
[89] F. Verstraete, J. J. García-Ripoll, and J. I. Cirac, Matrix product density operators: Simulation of finite-temperature and dissipative systems, Phys. Rev. Lett. **93**, 207204 (2004).
[90] J. Cui, J. I. Cirac, and M. C. Bañuls, Variational matrix product operators for the steady state of dissipative quantum systems, Phys. Rev. Lett. **114**, 220601 (2015).
[91] H. P. Casagrande, D. Poletti, and G. T. Landi, Analysis of a density matrix renormalization group approach for transport in open quantum systems, Comput. Phys. Commun. **267**, 108060 (2021).
[92] D. Wellnitz, G. Preisser, V. Alba, J. Dubail, and J. Schachenmayer, Rise and fall, and slow rise again, of operator entanglement under dephasing, Phys. Rev. Lett. **129**, 170401 (2022).
[93] M. Žnidarič, Entanglement in a dephasing model and many-body localization, Phys. Rev. B **97**, 214202 (2018).
[94] E. V. Doggen, I. V. Gornyi, A. D. Mirlin, and D. G. Polyakov, Many-body localization in large systems: Matrix-product-state approach, Ann. Phys. **435**, 168437 (2021).